Composites: Part A 41 (2010) 774–786

Contents lists available at ScienceDirect

Composites: Part A

journal homepage: www.elsevier.com/locate/compositesa

Predictive modeling of an energy-absorbing sandwich structural concept using the building block approach

Paolo Feraboli [a,*], Francesco Deleo [a], Bonnie Wade [a], Mostafa Rassaian [b], Mark Higgins [b], Alan Byar [b], Maurizio Reggiani [c], Andrea Bonfatti [c], Luciano DeOto [c], Attilio Masini [c]

[a] Dept. of Aeronautics & Astronautics, University of Washington, Seattle, WA, United States
[b] Boeing Research & Technology, The Boeing Co., Seattle, WA, United States
[c] Research & Development, Automobili Lamborghini S.p.A., Sant'Agata Bolognese, Italy

ARTICLE INFO

Article history:
Received 8 August 2009
Received in revised form 30 January 2010
Accepted 23 February 2010

Keywords:
A. Carbon fibre
A. Honeycomb
B. Impact behaviour
C. Finite element analysis

ABSTRACT

An energy-absorbing composite sandwich structural concept, comprised of a deep honeycomb core with carbon/epoxy facesheets, is subject to through-thickness crushing and penetration using a cylindrical pole. With the aid of the building block approach, the response of the structure is predicted by analysis supported by test evidence. Experiments are conducted at various levels of complexity, from the coupon level used to generate material properties to be used as input in the finite element models, through the element level used to calibrate the analysis models, and up to the component level to validate them. LS-DYNA is used to perform the analyses, including material models MAT 54 for the facesheets, MAT 126 for the honeycomb, and tie-break contact for the adhesive. Material models and contact formulations require extensive calibration of modeling parameters at the lower and intermediate levels of the building block pyramid, but eventually enable the prediction of the full-scale structure.

1. Introduction

1.1. Building block approach, or certification by analysis supported by test evidence

Currently, the large commercial transport aircraft industry utilizes a certification approach known as "certification by analysis supported by test evidence", or "allowables-based certification", to demonstrate compliance with regulatory Agency requirements, such as those of the Federal Aviation Administration (FAA). Margin of Safety calculations for static strength, durability and damage tolerance of composite materials are based on a complex mix of testing and analysis. This substantiation process is known as the Building Block Approach (BBA) [1,2]. In the commercial aircraft industry, it is recognized that analysis techniques alone are not sufficiently predictive for composites. However, by combining testing and analysis, analytical predictions are validated by test, test plans are guided by analysis, and the cost of the overall effort is reduced, while the degree of confidence and safety is increased.

The BBA is comprised of analyses and associated tests at various levels of structural complexity, often beginning with small coupons and progressing through structural elements, sub-components, components, and finally the complete full-scale product (Fig. 1, left). Each level builds on knowledge gained at previous, less complex levels. Progressing upward on the pyramid, specimen complexity and cost increase, as well as the degree of specificity of the test, but the number of tests decreases. Tests at the lower levels of the pyramid are conducted to generate the material properties to feed the appropriate analysis methods. These can include as many as 8000 coupon level tests for a new airplane program. Moving up in the pyramid, at the element level, tests are used to calibrate the analysis methods previously generated. This includes "tweaking" some modeling parameters that may not be measured experimentally, and hence need to be fitted to the specific configuration being designed. At the highest levels of the pyramid,sub-component or full-scale component levels, tests are used exclusively to validate the analysis methods previously calibrated.

To date, the complexity associated with crash modeling of composite structures has been one of the most limiting factors in the widespread introduction of composites in the mainstream automotive industry [3]. This study proposes to utilize the BBA, widely used in the aerospace community but often not utilized in the automotive industry, for the certification by analysis sup-

* Corresponding author. Address: Automobili Lamborghini Advanced Composite Structures Laboratory, Dept. of Aeronautics and Astronautics, Box 352400, Guggenheim Hall, University of Washington, Seattle, WA 98195-2400, United States.
E-mail address: feraboli@u.washington.edu (P. Feraboli).

1359-835X/$ - see front matter © 2010 Elsevier Ltd. All rights reserved.
doi:10.1016/j.compositesa.2010.02.012

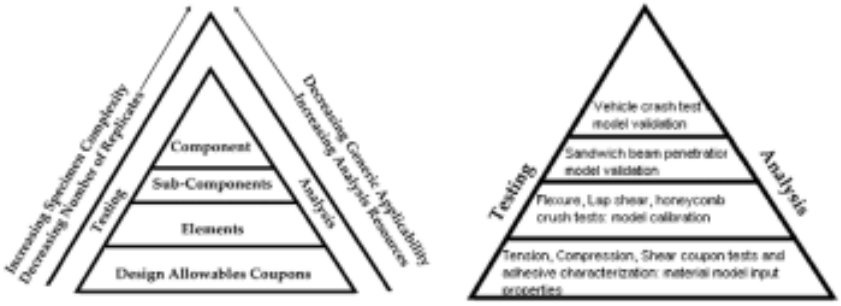

Fig. 1. Generic building block approach (left), and its application to the current study (right).

ported by test evidence of an energy-absorbing structural concept for a high performance vehicle. Using this approach, it is shown that certification by analysis can be used successfully for simulating composite crushing and penetration.

1.2. Material models for simulating progressive damage of composite materials

Finite Element (FE) modeling of the failure initiation and propagation in composite materials is a challenging task, and one that becomes even more complex if the response is time-dependent as in the case of crash simulations. The large deformations of the material/structure under crash conditions are often, if not always, associated with impact loading. Mathematically, the problem is described by the equations of motion, which are typically solved numerically by direct integration using explicit, rather than standard (or implicit), methods. These calculations are computationally expensive, and are often limited by available computational resources. Furthermore, within a large aircraft or automotive corporation, a specialized set of skills is required for the engineers that perform crash or similar dynamic analyses.

Dynamic failure simulations are extremely difficult to run, require extensive calibration, and the results are known to vary depending on the computer platform or processing power employed [3]. These models are also known to be highly mesh-dependent; hence selection of the element size and distribution is very difficult. Lastly, since crash simulation inevitably involves the use of one or multiple types of contacts between the components involved in the event, selection of the contact type is also fundamental. The calibration is based on the use of parameters that can be either associated to a measurable material property, or to mathematical parameters pertaining to the specific FE code utilized, which have either no physical meaning or they cannot be measured experimentally. These parameters need to be estimated based on previous experience and a trial-and-error approach [3–5]. Because of the extensive calibration needed, explicit dynamic simulations, such as those used to model crash events, hail or bird strike damage, and foreign object impact damage, have the reputation of requiring the utilization of "tweaking" parameters, sometimes negatively referred to as "fudge" factors, to achieve the desired level of accuracy in reproducing experimental results. The results obtained are rarely predictive and are typically used to "match" previously generated experimental data.

The computational cost associated with the use of 3D solid elements is often prohibitive in explicit dynamic simulations, and 2D shell elements are commonly used. For similar reasons, joints between composite components, whether adhesively bonded or fastened, are typically simulated using simplified "tie-break contacts" or "spot welds" [6]. These expedients reduce the ability to closely represent the geometric and physical problem but, if properly calibrated, have the potential to capture all relevant physical and engineering responses. In commercially available FE codes used for explicit dynamic simulations, a library with existing material models, also referred to as "material cards", is often available [6]. These material models comprise a set of parameters that go beyond the material properties required to characterize the behavior of the material being simulated. They generally include the definition of a failure criterion, to determine the initiation of damage, and of the degradation algorithm required to model the propagation of such damage. The ability of a FE code to successfully model the crash problem at hand is highly dependent on the suitability of the material model to capture the failure response of the material under crash conditions.

Composite constitutive models implemented in commercial explicit FE programs are continuum mechanics models. Composites are modeled as orthotropic linear elastic materials within a failure surface. The exact shape of the failure surface depends on the failure criterion adopted in the model. A variety of failure criteria have been developed for laminated composites. The common failure criteria implemented in composite material models in commercial codes are typically strength based, such as Tsai-Wu, Hashin, and Chang–Chang [3,6]. Beyond the failure surface, the appropriate elastic properties are degraded according to degradation laws. Depending upon the specific degradation law used in a model, the continuum mechanics models can be further divided into either progressive failure models or continuum damage mechanics models. Progressive failure models use a ply discount method to degrade material properties. At the failure surface, the values of the appropriate elastic properties of the ply in the material direction are degraded from its undamaged state to a fully damaged state, which is often considered a complete loss and assigned a value of zero. Progressive failure is realized through ply-by-ply failure in the perspective of a laminate. Continuum damage mechanics models describe the collective influence of distributed defects and their evolution on the stiffness and strength of the material through the use of internal state variables, commonly known as damage parameters. In this study, only progressive failure models will be employed.

Only a few commercial explicit codes are available for simulating the crash response of composite materials, and include Altair's RADIOSS, Simulia's ABAQUS Explicit, ESI's PAM-CRASH, and LSTC's LS-DYNA [3]. Since 2004, the CMH-17 (former MIL-HDBK-17) Crashworthiness Working Group has been promoting the development of both standardized test methods for measuring composite crash energy absorption, and numerical analysis guidelines for creating successful and reliable FE models [3]. Toward that extent, a large round robin exercise has been initiated to assess the strengths and limitations of available modeling strategies, such as material models and contact definitions, of commercially available FE codes. Representatives from software companies and experienced users in the aerospace and automotive industries are involved in this exercise [3]. LS-DYNA, being the oldest available code among the ones mentioned, has traditionally been considered

the benchmark for composite crash simulations. Table 1 shows the material models available in LS-DYNA to model damage initiation and propagation in composite materials. The following discussion will show how specific material models and contact algorithms in LS-DYNA are here selected to simulate the various components of the structure considered. These include the use of a "MAT 54 Enhanced Composite Damage Model" to simulate the carbon/ epoxy laminate facesheets, "MAT 126 Metallic Honeycomb" to simulate the aluminum honeycomb core, and "tie-break contact/interface definition" to simulate the adhesive bonding between facesheets and core.

Each of the material models used in this study requires different input parameters, some of which can be directly measured by specific experiments, and others that are determined by trial-and-error. Few, if any, sources are available to help in selecting the appropriate parameters, and the success of the simulation is almost exclusively based on the experience of the user. The purpose of this paper is to show that the building block approach, utilized in the aerospace Industry to design, analyze and certify structural components for static strength as well as durability and damage tolerance, can be utilized successfully for crashworthiness, both in the aerospace and automotive communities.

1.3. Oblique pole crash test in the new side impact protection safety standard

Traditionally, the Federal Motor Vehicle Safety Standard (FMVSS) No. 214 [7] has included two tests to assess the ability of a vehicle to provide safety for its occupants during a side impact. The first test, "Door Crush Resistance Requirements", uses a 12 in. (304.8 mm) diameter instrumented rigid steel cylinder, which is pushed at quasi-static rate into the vehicle door. The cylinder is sized so that it intrudes the door structure alone, without contacting the neighboring doorsill, A- and B-pillars, or the roofline. This test provides an assessment of the structural response of the door and its surrounding area, by showing compliance with specific minimum requirements on load and displacement characteristics, hence energy absorbed. The second test, "Moving Deformable Barrier Requirements", consists of a dynamic crash test where a trolley is launched against the stationary test vehicle and impacts it perpendicular to its centerline. Test speed is 33.5 mph (53 km/h). The barrier is comprised of an aluminum honeycomb bumper, mounted on an aluminum honeycomb block, which impacts a large portion of the vehicle side, spanning almost from the front to the rear wheel well area. The deformable barrier impact simulates the lateral impact of a car against another vehicle. This test focuses on assessing the forces and accelerations measured on anthropomorphic test dummies. Therefore the results are not influenced by the structural performance alone, but by the vehicle as a whole, including restraint systems.

Recently, a third test has been added, "Oblique side pole impact test", which assesses the ability of a vehicle to protect its occupants during a sideways crash into a fixed utility pole or tree [8]. The test requires the vehicle to be launched at 20 mph (32.2 km/h) against a 10 in. (254 mm) diameter fixed rigid steel pole. The centerline of the pole is aligned at an angle of 75° from the longitudinal axis of the vehicle, and through the center of gravity of the driver dummy's head, Fig. 2. As in the deformable barrier side crash test, the success of this test is based on whether the forces, deflections, and accelerations measured on anthropomorphic dummies are contained within allowable limits. The overall success is influenced not only by the structural configuration, but that of the vehicle as a system. Nonetheless, this new requirement may significantly change the design of the structure surrounding the occupant in the proximity and even away from the impact location. The deformations introduced into the door, doorsill, and roofline by the large forces generated at impact have the potential to require dramatic changes in the design of the structure in future years.

The advent of composite-intensive chassis, such as carbon fiber monocoques, poses new challenges for the designer tasked with assessing the energy absorption of composite materials. The drive for increased power-to-weight ratio, achieved by reducing the overall weight of the vehicle, has pushed high performance car manufacturers toward the use of composite materials. This, in turn, leads to increased acceleration performance, better handling and dynamics, and reduced emissions. Production high performance vehicles are not exempt from today's stringent emissions regulations. Carbon fiber composites have shown to be able to perform extremely well in a crash, and are being used to manufacture dedicated energy-absorbing components. Examples in the motorsport world are the nose, rear and side impact structures of a Formula 1 racecar, and in the aerospace world is the Boeing 787 crushable subfloor. Their ability to dissipate more energy per unit mass than aluminum or steel is however obtained only through a complex and careful design effort. This effort has been traditionally performed by experiment alone, by crash-testing actual components and evaluating different structural concepts. This practice is costly and time-consuming, and results in very large experimental programs to ensure the correct performance of the component under varying load scenarios. Furthermore, full-scale crash tests involve the manufacturing of a full-scale prototype, and are typically performed well into the program, after the overall design of the vehicle has been frozen. Unsatisfactory crash performance can lead to dramatic changes in the design of the vehicle, which in turn can result in delays, additional costs, and possible weight penalties. A reliable simulation tool is needed to predict the crash response of the structure during the design stage and well before full-scale crash testing.

To limit the forces transmitted to the occupant and the deformations of the occupant compartment during the new oblique side pole impact, new structural concepts (Fig. 3) are being studied. The concept is to absorb as much energy as possible in the doorsill area, where structural volume is available, rather than in the door or in the roofline. In this study, a composite sandwich structure, comprised of carbon/epoxy facesheets with an aluminum honeycomb core, is selected to demonstrate its ability to absorb energy. The test seeks to obtain a desired force–displacement curve, which is indicative of the force transmitted to the floor (which support the seat attachment points) and of the intrusion into the passenger compartment. The test also seeks to generate a desired force–time impulse, which is necessary for the exact deployment of the lateral airbag system. Typically this effort would be conducted experimentally by running multiple full-scale crash tests. Sometimes full-vehicle FE models are used to match and support the results after the tests are performed. This study shows that it is possible to utilize a predictive approach based on analysis supported by test evidence gathered at element and sub-component levels. Using the BBA, the analysis predictions result in the confidence to reduce the number of full-scale crash tests to be performed, with the understanding that final vehicle certification can still be achieved by full-scale crash testing. This study shows the development through

Table 1
Summary of composite material models available in LS-DYNA.

MAT	Title	Brick	Shell	Degradation law
22	Composite damage	y	y	Progressive failure
54/55	Enhanced composite damage		y	Progressive failure
58	Laminated composite fabric		y	Damage mechanics
59	Composite failure	y	y	Progressive failure
161	Composite MSC	y		Damage mechanics
162	Composite MSC	y		Damage mechanics

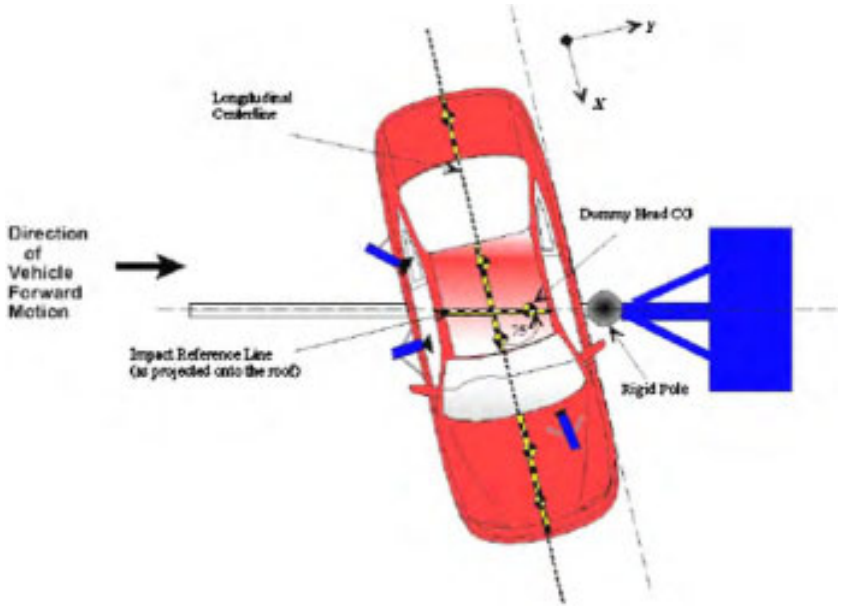

Fig. 2. Illustration of oblique pole side crash test [8].

the BBA of the composite energy-absorbing concept, and stops short of the full-scale vehicle crash simulation and testing. These results are not provided because they involve several non-structural considerations, such as airbag and dummy responses, and can infringe on proprietary issues.

2. Experiment

2.1. Materials and fabrication

The doorsill structural concept is a sandwich fabricated of composite facesheets, honeycomb core and film adhesive. The structure is 37.8 in. (960 mm) long, 7.87 in. (200 mm) wide, and 7.87 in. (200 mm) thick. In the vehicle, the structure spans from A-pillar to B-pillar, and is oriented sideways, with one facesheet oriented outward, and the other oriented toward the passenger compartment. The rigid pole impacts the outer facesheet, penetrates into the core for up to 80% of its depth, but does not intrude into the inner facesheet. Although the part has a complex geometry, tapering both in width and height from the front of the vehicle to the back, it can be idealized as a flat beam resting against a rigid, flat surface being intruded midspan by the rigid pole.

The facesheets are comprised of a carbon fiber fabric Toray T700 2 × 2 Twill, 12 k Tow, 380 gr. and a Cytec 977-6 highly toughened epoxy resin. The prepreg lamina has nominal thickness 0.016 in. (0.4 mm) and 58% fiber volume. The facesheets are cured as separate laminates in the autoclave, according to manufacturer specification, using peel ply on the side where bonding will take place. Curing takes place at 275 °F (135 °C) and 100 psi (6.89 bar) for 3 h. Cured laminate thickness is 0.157 in. (4.0 mm). The honeycomb core is 5056 aluminum alloy, with 0.125 in. (3.2 mm) hexagonal cell size, 0.001 in. (0.03 mm) cell wall thickness, and 4.5 pcf (72 kg/m^3) density. Hexcel Corp supplies the core. The adhesive joint is realized with a modified epoxy film adhesive, Cytec FM87-1, of nominal thickness 0.010 in. (0.25 mm). Surface preparation is obtained by sanding the composite facesheet, after removal of the peel ply, followed by cleaning with alcohol and drying. Bonding takes place in the autoclave at 250 °F (121 °C), 30 psi (2.07 bar) pressure, and for a duration of 1 h.

2.2. Coupon level tests

Several tests, of varying complexity and cost, are performed along the allowable, element and sub-component levels of the BBA pyramid (Fig. 1, right). Properties measured in the laboratory rather than the supplier data are used to generate the input values for the respective material models. At the lower level of the building block, the allowable level, the composite facesheets alone are tested. Tension, compression, in-plane shear coupon tests are used to characterize the moduli, strengths, and strains-to-failure of the facesheets at quasi-static test rates. ASTM standard test methods D3039 (unnotched tension) [9], D6484 (unnotched or open-hole compression) [10], and D5379 (Iosipescu shear) [11] are used to generate the lamina properties. The results are summarized in Table 2. Specimens and associated test fixtures and set-ups are shown in Fig. 4. With these properties, it is possible to generate all input data necessary for generating the MAT 54 material card used to simulate the facesheets. No properties are measured at this level for the honeycomb core or the adhesive, since the respective material models, MAT 126 and tie-break contact interface, do not require them. The properties of the core and of the adhesive are reported in Tables 3 and 4, respectively for information purposes.

2.3. Element-level tests

Progressing up the BBA pyramid, element-level tests are performed on specimens that are already specific to the structural configuration of the energy absorber concept. Moreover, the purpose of these tests is not to generate input material properties for the material models, but to generate specific load–displacement curves to be used to calibrate the material models.

For the facesheets, a three-point bend flexure test is performed according to ASTM standard D790 [12] at a quasi-static loading rate of 1.0 in./min (25.4 mm/min). The specimen being loaded in the dedicated test fixture is shown in Fig. 5, and has dimensions 6.5 in. long (165.1 mm) × 1.0 in. wide (25.4 mm) × 0.157 in. thick (4 mm). The value of flexural strength obtained is not used as input for the MAT 54 card. However, the load–displacement curve obtained during this test is used for calibration of the MAT 54 mate-

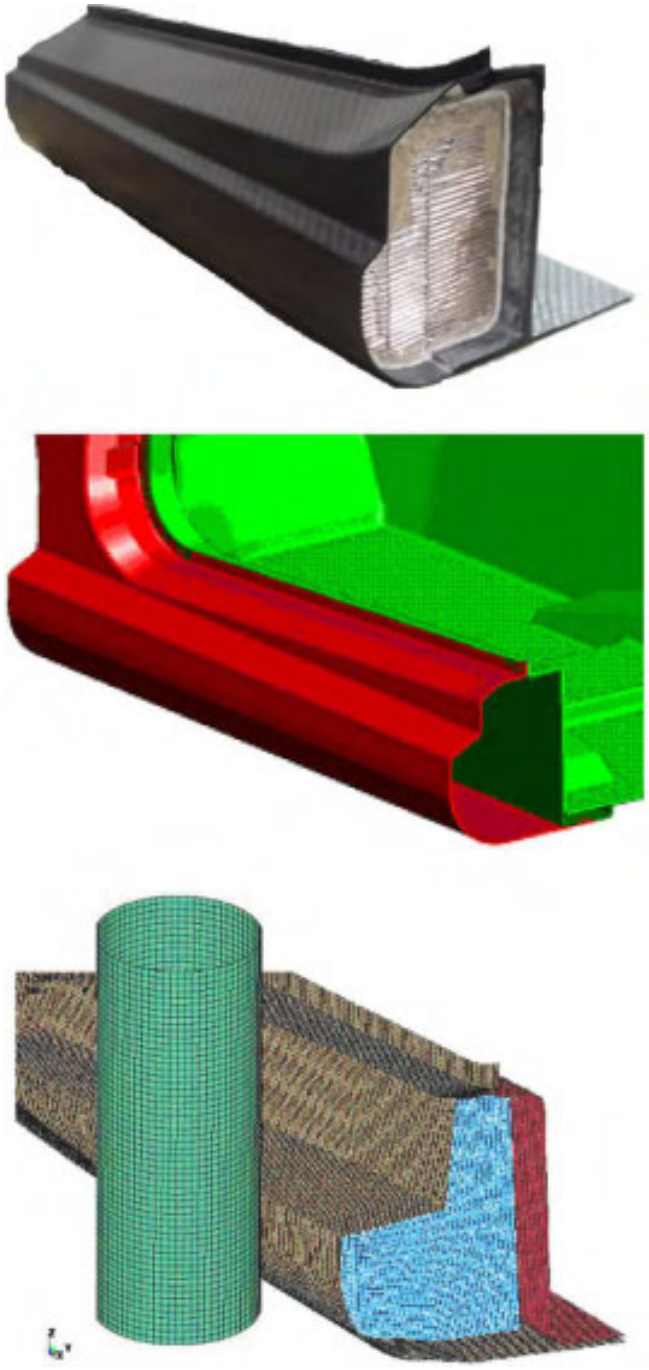

Fig. 3. Section of the vehicle structure corresponding to the side doorsill, including the energy-absorbing concept.

Table 2
Measured T700/977-6 facesheets laminate properties.

Measured	Stacking sequence	$E_x = E_y^{tens}$ [Msi] (GPa)	$E_x = E_y^{comp}$ [Msi] (GPa)	G_{xy} [Msi] (GPa)	ν_{xy}
Laminate	$[(0/90)]_{10T}$	8.9 (61.35)	7.4 (51.01)	0.55 (3.79)	0.043
	Stacking sequence	$F_1^{tu} = F_2^{tu}$ [Msi] (GPa)	$F_1^{cu} = F_2^{cu}$ [Msi] (GPa)	F_{su}	
Laminate	$[(0/90)]_{10T}$	118.8 (819.1)	77.2 (532.3)	16.1 (111)	

rial card, since the strain-to-failure in the model needs to be "tweaked" by trial and error in order to achieve good correlation between simulation and experiment.

For the honeycomb, a stabilized core crush test [13] at quasi-static loading rate of 1.0 in./min (25.4 mm/min) is performed according to ASTM standard D7336 [13] to generate the load–displacement curve. The specimen has dimensions 4.72 in. long (120 mm) × 4.72 in. wide (120 mm) × 7.87 in. thick (200 mm). The test curve is used as input in the MAT 126 material model. It will be seen that, unlike for MAT 54, this empirical material model relies purely on load–displacement data generated experimentally. The model does not have the power to produce a predicted load–displacement curve based on the material properties of the aluminum core. The progression of the crush is shown in Fig. 6, together with the final shape after full compaction. For the adhesive, single-lap shear tests are performed at a quasi-static loading rate according to ASTM standard D1002 [14], using two identical composite factsheets. Each of the two specimens has dimensions are 6.0 in. long (203.2 mm) × 0.5 in wide (12.7 mm) × 0.157 in. thick (4.0 mm). Fig. 7 shows the specimen before and after failure, and indicates that successful cohesive failure is achieved.

The importance of generating user-specific properties is also to measure the in situ, as manufactured properties of the materials considered. For the honeycomb, the effect of core depth, which in this case is several times that of the core used to generate material properties declared in the supplier datasheet, can be substantial in affecting the crush strength. For the bonded joint, the effect of adherend thickness, material system and surface preparation can have great effect on the measured strength, thus relying on supplier data can lead to erroneous simulation results.

2.4. Sub-component level tests

A flat sandwich beam of the same size of the door sill component is manufactured and subjected to quasi-static penetration/crushing using a steel pole identical to the one used in the full-scale crash test, Fig. 8. The beam rests on a fixed, rigid steel surface and is free to rotate. The morphology of failure for the beam is shown in two different instants during the penetration in Fig. 9. The boundary conditions of the test configuration attempt to represent the conditions of the component in the vehicle as close as possible, with the inner facesheet constrained from deforming inward and intruding into the passenger compartment. This test is used to generate a load–displacement curve, which is used exclusively to validate the assembly-level FE model. At this level, the model needs to be fully predictive; hence it shall no longer be calibrated or "tweaked". Any subsequent modification, even if required to match experimental data, would result in the loss of ability to use the model as a predictive tool. The experimental curve can also be integrated to yield a reference value for energy absorbed, which gives an indication for how much energy could be dissipated by the doorsill and not transferred to the rest of the vehicle during the crash test.

2.5. Component level tests

The final step in the BBA requires a global vehicle model crash simulation, and its associated validation via full-scale vehicle crash test. Both simulation and test need to be performed according to the new FMVSS No. 214 [8], and therefore involve the vehicle as a whole, including chassis and body panels, doors, windows, passenger restraint systems, dummies, etc. If further instrumentation is added to the test (e.g. local accelerometers and high-speed cameras) it is then possible to extrapolate from the full-scale crash test

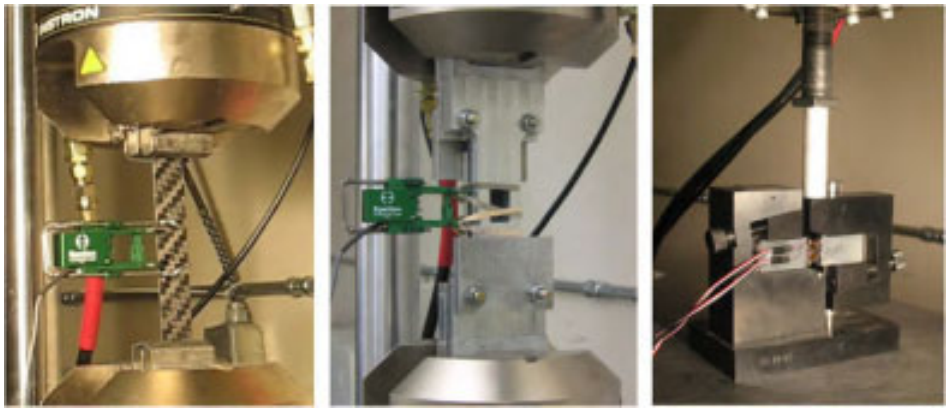

Fig. 4. Coupon level tests performed on the facesheet material include tension, compression and in-plane shear.

Table 3
5056 Aluminum honeycomb core properties.

	Compressive strength [psi] (MPa)	Modulus [ksi] (MPa)	Crush strength [psi] (MPa)
Supplier data	690–500 (4.76–3.45)	185 (1,275)	320 (2.21)
Measured data	556 (3.83)	–	324 (2.23)

Table 4
FM87 Adhesive properties.

	Lap-shear strength [psi] (MPa)	Flat-wise tensile strength [psi] (MPa)
Supplier data	5490–3890 (37.8–26.8)	1050 (7.24)
Measured data	3710 (25.6)	–

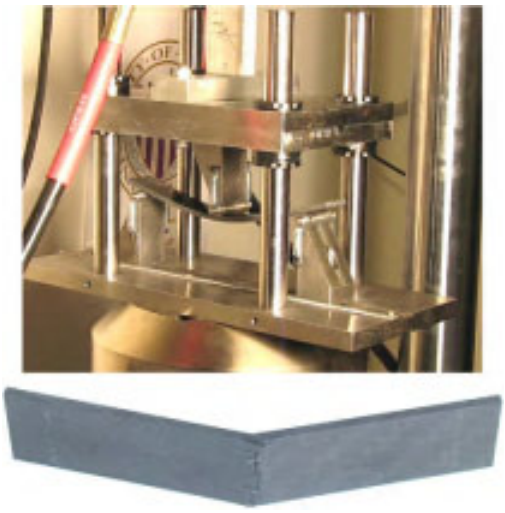

Fig. 5. Three-point bend flexure element-level test: specimen in the test fixture being loaded (top) and after failure (bottom).

the structural behavior of an individual sub-component, such as the configured doorsill. Detailed description of both simulation and test are very complex and proprietary, and will not be included in this discussion.

3. Simulation

3.1. MAT 54 for the composite facesheets

The composite facesheets are modeled using MAT 54 in LS-DYNA, which is a progressive failure model for shell elements that utilizes a highly modified version of the Chang–Chang failure criterion [6]. The failure criterion is based on the single lamina strengths in tension, compression and shear, in both the axial and transverse directions. When the resolved stress state within an individual lamina exceeds the strength, the lamina is deleted, but the element is still active. The element is deleted only when all laminae reach failure. When an element reaches failure, it is eroded and it simply disappears. The failure morphology for MAT 54 is of little graphical interest, as it does not exhibit frond formation or fragmentation as does, for example, MAT 58. Beside the strength-based failure criterion, a lamina can also fail if one of the strains reaches a critical value [6].

The model requires the input of several material properties for the single lamina: density, Young's moduli and shear moduli in three directions, strength in tension and compression in longitudinal and transverse direction, shear strength, strain-to-failure of the lamina in tension, compression and shear, and strain to failure of the matrix alone. All of these parameters, except for the last one, which is supplied by the resin manufacturer, are obtained here though coupon-level testing.

Several other parameters are of importance in MAT 54, such as the α and β parameters, which are constants used in the definition of the failure criterion, and TFAIL, which is the time step criterion for element deletion. Lastly, the SOFT crush front parameter, was shown in [4] to greatly influence the axial crush simulation results. The force-penetration curve is a characteristic of the contact formulation and specifies the rate at which an element experiences contact with another body's element. It also prescribes the distance at which the element senses the contact with an approaching element, although physical contact may not have yet occurred. These last five quantities cannot be measured experimentally, and are typically adjusted by trial and error. In order to do so, the three-point bend flexure test is reproduced in LS-DYNA, with the goal to manually calibrate these parameters in order to achieve a successful match between experiment and simulation.

The 10-ply laminate is modeled using a 0.1 in. $\times$ 0.1 in. (2.5 mm $\times$ 2.5 mm) element size, for a total of 3335 shell elements. The support and loading rollers are modeled using solid tetrahedral elements, and are assigned steel material properties using MAT 20 [6]. The laminate rests on the support rollers, which are fixed in all degrees of freedom (dof) on their bottom surface. Contact between

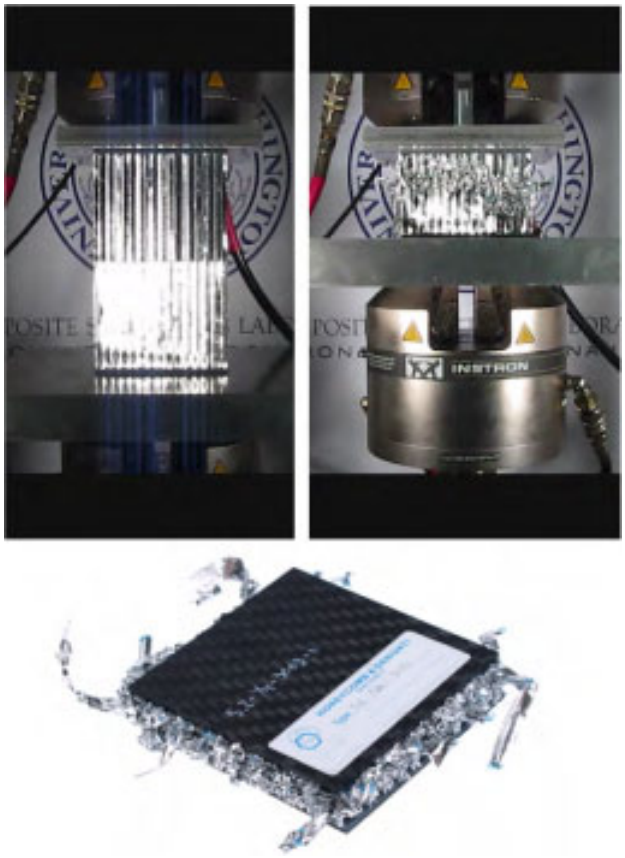

Fig. 6. Core crush element-level test, during the test (top) and at full compaction (bottom).

the laminate and the roller is achieved by means of the available contact definition "rigid_nodes_to_rigid_body". The loading roller is prescribed a constant velocity of 150 in./s (3.81 m/s). Although the experiments have been carried out at the quasi-static rate of 1 in./min (25.44 mm/min), all simulations are executed at 150 in./s (3.81 m/s). The computational power required to perform these simulations at quasi-static rates far exceeds the one available to most explicit FE users. A compromise between computational time and the physical test has been found to be 150 in./s (3.81 m/s). It is possible that the dynamic effects associated with the dynamic speeds used in the simulations can introduce inertial effects not visible in the quasi-static experiments. However, strain-rate dependent phenomena should not be cause of concern since the material uses quasi-static material properties and does not accommodate for strain-rate behavior in the input parameters. An SAE 600 Hz filter is used to smooth out the oscillations due to vibration. The model at the beginning and end of the simulation is shown in Fig. 10.

Several attempts are made to adjust the five quantities discussed above, but with little success. The simulation invariably results in an accurate predicted load (hence strength), but much lower displacement at failure, thus resulting in a virtually stiffer load–displacement curve. It is found during the investigation that the SOFT parameter has, for this condition only, no significant effect on the results. By adjusting the material card, in particular by artificially increasing the strain to failure in tension and compression, by as much as a factor of two or three, using an idealized elastic-perfectly plastic curve (Fig. 11), a perfect match between the experimental and numerical load–displacement curve is achieved (Fig. 12). In Fig. 12, three different experimental curves are reported, to show that a certain degree of variability is present also among experimental data. This modification, which has no physical meaning, can appear at first shocking to researchers used to performing FE modeling in the elastic range. However, calibration efforts of this kind are necessary when dealing with post–elastic FE models. The difference in predicted load–displacement curves between the original material stress–strain curve in tension and compression, and the modified one are also shown in Fig. 12. It

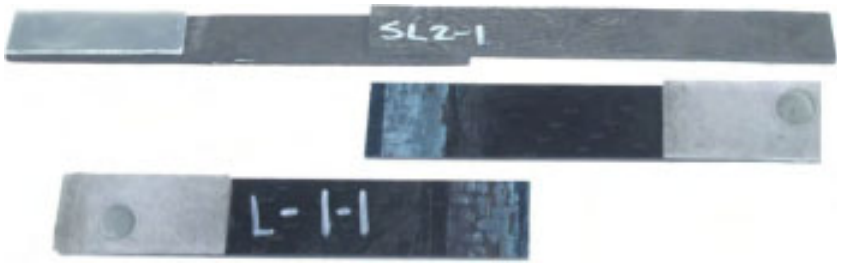

Fig. 7. Single-lap shear element-level test for the adhesive, before (top) and after failure (bottom).

Fig. 8. Subcomponent level test of the full assembly being penetrated by the pole at two different instants during the test.

Fig. 9. (Top) Partially crushed morphology of the assembly – test was interrupted to take picture. (Bottom) Final morphology of the assembly after testing.

can be seen how the fictitious plastic strain plateau has the effect of extending the specimen's ability to deform up to the necessary displacement value. The low frequency oscillations visible in the numerical curve are due to the dynamic nature of the simulation, and are not present in the quasi-static test data. Both numerical predicted curves are slightly shifted to the left of the origin, and the reason is associated with a thickness offset between the parts, necessary for the contact definition.

3.2. MAT 126 for the metallic honeycomb core

The aluminum honeycomb is modeled using MAT 126 in LS-DYNA, which is an orthotropic elastic–plastic model used for solid (brick) elements. The hexagonal cell structure of the honeycomb is thus represented by means of a homogeneous solid element with orthotropic properties. The magnitude of the components of the stress tensor are defined by load–displacement curves, which need to be experimentally generated and input to the model. Failure is reached when the element's stress components under load exceed the permissible values dictated by the empirical load–displacement curves.

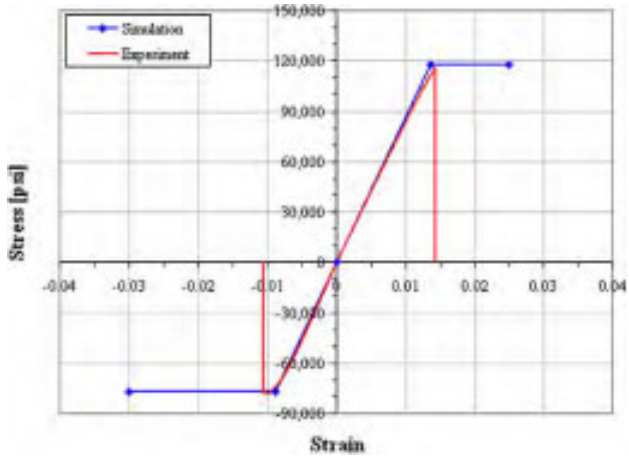

Fig. 11. Tensile stress–strain curve for the facesheet material, as measured from the experiment and in its final modified version for the simulation.

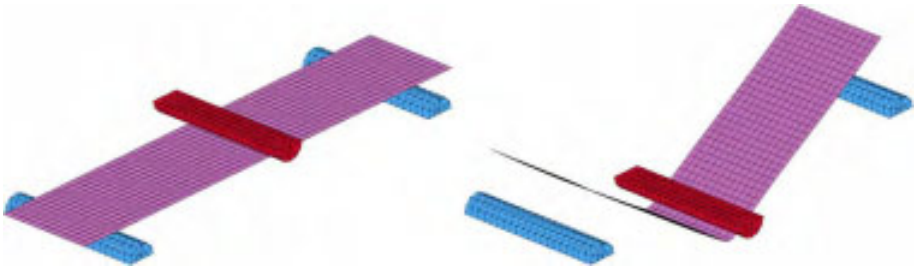

Fig. 10. Three-point bend flexure element-level simulation of the facesheets, at the beginning (left) and the end (right) of the loading.

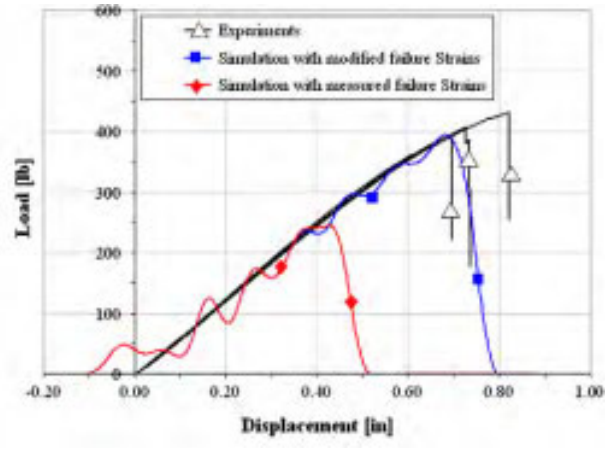

Fig. 12. Comparison of experimental and simulated three-point bend flexure load–displacement curves, of which one uses the measured strain-to-failure, the other the modified version of Fig. 11.

The model requires the input of the experimental load–displacements curves, obtained by axial crushing of the stabilized honeycomb element previously discussed. The core requires both uncompacted and compacted material properties. Therefore, it is necessary to run the test to full compaction in order to obtain all values of strength and modulus, since the model requires both compacted and uncompacted core material properties. The model also requires the input of several material properties for the honeycomb, such as: modulus and yield strength after compaction, and elastic moduli in all directions before compaction. These properties can be obtained from the manufacturer. To validate the model, the honeycomb crush test is reproduced numerically in LS-DYNA, using 0.1 in. × 0.1 in. (2.5 mm × 2.5 mm) elements, for a total of 1600 hexahedron (brick) elements. The loading plate is modeled using 887 solid tetrahedral elements of MAT 20. The honeycomb's boundary conditions call for the bottom row of elements to be fixed along the vertical (axial) displacement. Contact between the honeycomb and the plate is defined by means "rigid_nodes_to_rigid_body". The loading plate is prescribed a velocity of 150 in./s (3.81 m/s). An SAE 600 Hz filter is used to smooth out the oscillations due to vibration. The model is extremely stable and, unlike the MAT 54 model of the facesheets, is very robust with respect to variations of model parameters. The model at the beginning and end of the simulation is shown in Fig. 13, while the comparison between experimental and numerical curves is shown in Fig. 14. As it can be seen, the model shows high accuracy in predicting the response of the material, but it should be emphasized that in order to obtain this result it is necessary to input the actual experimental curve into the material card.

A last consideration should be made with respect to the definition of modulus. The LS-DYNA theory manual [6] is, in the authors' opinion, too general at best to provide detailed information on the use of this material model. The modulus to be inserted in the material card for the compacted material is not the Young's modulus of the aluminum, but is rather the slope of the experimental stress–strain curve that is input in the card. In this study, a value of 0.5 is used rather than 10 Msi (3.45 GPa and 69 GPa, respectively). Similarly, the moduli of the honeycomb before compaction also correspond to the slope of the stress–strain curve obtained from crushing the honeycomb. This is obtained by dividing the applied stress (calculated as applied load/cross section area) by the nominal elongation. In this study for example, the measured value is therefore much smaller (0.97 Msi or 6.7 GPa) than the modulus of the aluminum alloy itself (10 Msi or 69 GPa), and this can be discovered only by experiment and trial-and-error.

3.3. TIE-BREAK contact for the adhesive

The adhesive joint between facesheets and core is modeled using the tie-break contact definition, which is used to tie the edges of adjacent shells together [6]. The master and slave nodes are tied by means of a normal and a shear mathematical relationship, which needs to be input in the model. These are obtained by supplying the shear and normal failure stresses of the adhesive. In this investigation, only the single-lap shear test is generated experimentally, while the normal or peel strength is based on the supplier data. Several other numerical parameters are needed for the definition of the model, such as the PARAM parameter, which is the strain-to-failure of the adhesive, and the closely connected OPTION parameter, which also needs to be set to the correct numerical value to enable OPTION to be active. In general, the technical information required for calibrating these parameters is simply not available in the LS-DYNA theory manual.

In order to validate the tie-break contact definition, the single-lap shear test between two composite adherends is reproduced in LS-DYNA. The model uses a total of 1100 of 0.1 in. × 0.1 in. (2.5 mm × 2.5 mm) shell elements for the MAT 54 adherends, whose material card is defined as specified in the case of the three-point bend flexure. The single lap joint is modeled as having one end fixed in all dof's for the 2.0 in. (50.8 mm) length of the grip

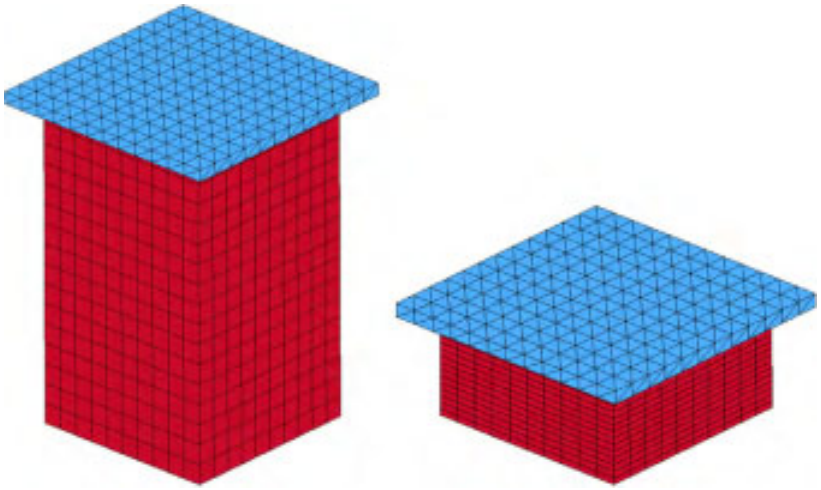

Fig. 13. Core crush element-level simulation, at the beginning (left) and the end (right) of the loading.

area, while the other is prescribed to be displacing at a velocity of 150 in./s (3.81 m/s) as in the previous cases. For the tie-break contact, the average measured shear strength of 3710 psi (25.58 MPa) is assigned, while the supplier provided peel strength of 1050 psi (7.24 MPa) is used. An SAE 600 Hz filter is used to smooth out the oscillations due to vibration. The model at the beginning and end of the simulation is shown in Fig. 15, while the comparison between experimental and numerical load–displacement curves is shown in Fig. 16. Four different experimental curves are reported, to show that a certain degree of variability is present in the experimental data. As it can be seen, the model shows high accuracy in predicting the response of the adhesive.

By trial and error, it is found that only the "Automatic_One_Way_Surface_To_Surface_Tiebreak" contact formulation works well for the case study at hand, while the other available options such as "Automatic_Surface_to_Surface_Tiebreak", "Tiebreak_Surface_to_Surface", and "Tiebreak_Nodes_to_Surface and Tiebreak_Nodes_Only" either led to premature failure or did not fail at all. It is also highly recommended to use the same mesh size for master and slave surfaces, to avoid interpenetration. This recommendation imposes limitations on the number of available elements to be used to model either the core of the facesheets, which could be different, depending on the available computational power. Furthermore, it is found that mesh size for the MAT 54 adherends has a large effect on simulation results. Lastly, by trial and error it is found that the optimal PARAM value for the present simulation is an intermediate average strain-to-failure value obtained from the experimental evidence. When PARAM is left to the default value of zero, failure occurs very prematurely.

3.4. Model of full-scale assembly

Once the material cards and contact definitions for all entities are calibrated at the element level, the full-scale assembly model can be generated. This simulation, which corresponds to the subcomponent level in the BBA, needs to show predictive capabilities, and the experimental data should be used only for validation purposes. As mentioned earlier, to maintain the predictive capability and integrity of the model, the material cards and contact definitions can no longer be changed.

The model is comprised of a rigid surface, on which the deep sandwich beam rests, and the rigid pole, which penetrates the beam. The support plate is fixed in all dof's. The sandwich beam is comprised of facesheets, honeycomb core and adhesive, which are modeled using the MAT 54, MAT 126 material cards and tie-break contact as defined in the previous sections. MAT 20 is used to model the rigid pole and support plates. Loading rate is 150 in./s (3.81 m/s) as in the previous cases. "Rigid_Nodes_To_Rigid_Body" contact formulation is used between the pole and a portion of the top facesheet, while the "Automatic_Surface_To_Surface" contact is used between the bottom facesheet and the support plate. Solid six-node tetrahedral elements are used to

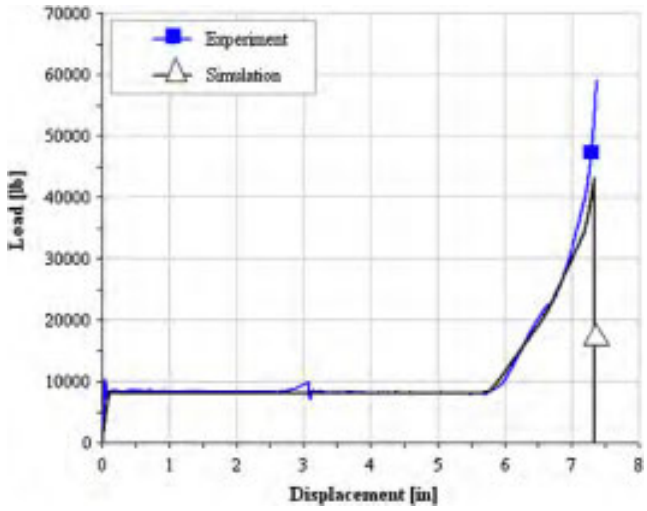

Fig. 14. Comparison of experimental and numerical core crush load–displacement curves.

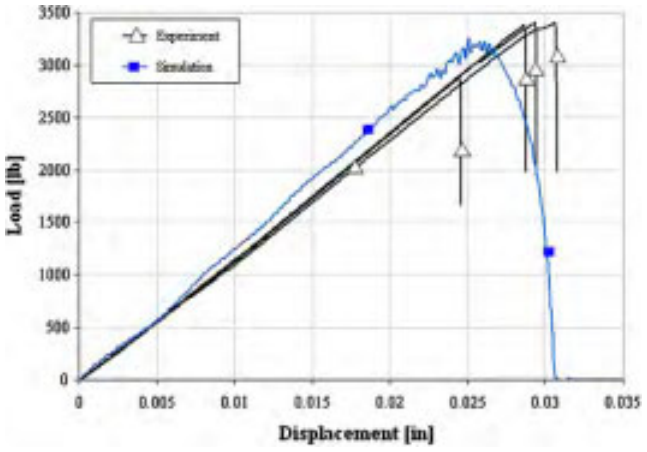

Fig. 16. Comparison of experimental and numerical single-lap shear load–displacement curves.

Fig. 15. Single-lap shear simulation of the adhesive, at the beginning (left) and the end (right) of the loading.

model the pole, four-node shells for composite facesheets and support plate, and solid eight-node hexahedrons for honeycomb core. A total of 26,271 elements are used, including 2783 tetrahedrons, 4032 shells and 19,456 hexahedrons. Mesh size for all surfaces is 0.5 in. × 0.5 in. (12.7 mm × 12.7 mm). This value is five times greater than the value used for the element-level simulations. This change is necessary because of the lack of more computational power to run the full-scale assembly simulations. Furthermore, the load to failure for the tie-break contact definition is reduced to 1/4 of the original values. This modification accounts for the difference in the surface area available in the facesheet-to-honeycomb joint and the surface available in the facesheet-to-facesheet single lap joint previously described, which is four times larger. In the tie-break contact definition, the load–displacement curve is used as input and not normalized by the area. Hence, the tie-break contact does not correspond to a true "strength" but to a "load-carrying capability", which needs to be normalized by the surface area.

Lastly, given the more complex stress state in the honeycomb core, which is now subject to combined axial crush and shear, requires the input of other load–displacement curves in the honeycomb MAT 126 formulation. Beside the already mentioned axial crush curve (or *z*-direction), additional normal load curves in the *x* and *y* directions, as well as shear curves in the *xy*, *xz* and *yz* directions are needed. Due to the complexity of testing such a deep honeycomb, these are not measured, but are taken from the literature [15,16] for a somewhat similar honeycomb core, and modified with available supplier data. These are the only three differences between the previous element-level simulations and this sub-component level model.

Three time steps during the progression of the crush simulation are shown in Fig. 17, at $t = 0$ s, $t = 0.0197$ s, and $t = 0.0399$ s, respectively. The comparison between experimental and numerical load–displacement curves is shown in Fig. 18. Good agreement is achieved between the two curves, with the simulation diverging slightly after 2.5 in. (63.5 mm) of crush. Compaction occurs at the same displacement for both the experimental and numerical curves, but at a higher load in the case of the numerical results. Overall, the total energy absorbed up to 3.0 in. intrusion (76.2 mm) is 8.07 kJ for the experiment and 8.63 kJ for the simulation, while at 6.0 in. (152.4 mm), right before compaction, it is 21.80 kJ for the experiment and 24.69 kJ for the simulation. The difference between prediction and experiments can be possibly explained by the behavior of the core. The left side of the core, Fig. 9, shears out and remains partially intact, thereby reducing the amount of energy absorption. The model unfortunately is not able to capture this difference between the left and right side, and therefore predicts slightly higher energy absorption. The progression of facesheet deformation, where the facesheets are not shown for better visualization, is given in Fig. 19, which also shows the evolution of longitudinal (axial) stresses during two of the three steps of Fig. 17.

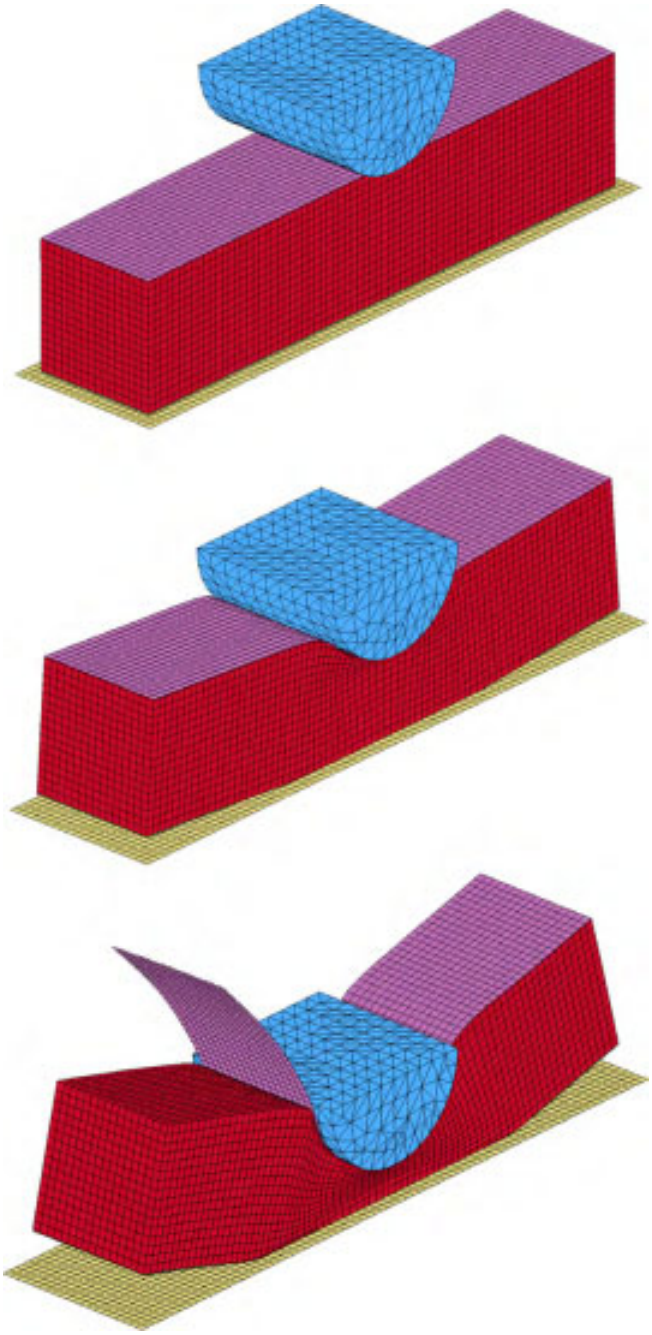

Fig. 17. Subcomponent level simulation of the full-scale assembly being penetrated by the pole, shown during three different time steps: $t = 0$ s, $t = 0.0197$ s, and $t = 0.0399$ s.

4. Discussion

The results of the full-assembly experiment and simulation are considered favorable. The disciplined effort followed by the authors to perform the calibration of the various material models and contact definitions has enabled a high degree of confidence in the predictive capabilities of the model. Scaling up to the actual component level configured doorsill within the global vehicle simulation can be performed with the confidence that all fundamental aspects of the simulations are well understood. Nonetheless, this achievement comes at a high price. Dozens of tests have been performed at the coupon level, a few at the element level, and one at the sub-component level. Over a hundred simulation trials have been performed at the element level, and a dozen at the sub-component level. Parameter sensitivity studies and trial-and-error simulations have been used to find optimal values for those parameters that either could not be measured experimentally or needed to be modified from the experimental ones in order for the simulation to run successfully.

For example, the load to failure of the tie-break contact used to simulate the strengths between facesheets and honeycomb were changed from those obtained experimentally on facesheet-to-facesheet joints. Although physically explainable, this change has not been validated by element level testing. Nonetheless, the simulation runs successfully both with the nominal strength values, as well as for the reduced values, 927 psi (6.4 MPa) and 262 psi (1.81 MPa), respectively. The effect on the load–displacement

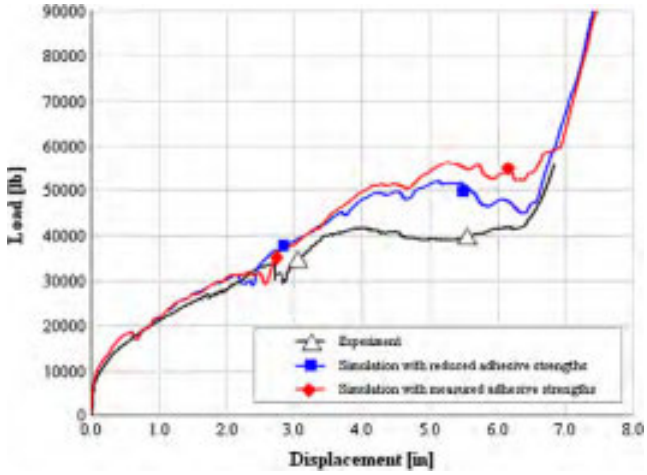

Fig. 18. Comparison of experimental and simulated assembly level test, of which one uses the measured adhesive strengths, the other the reduced set of strengths.

curves is shown in Fig. 18, and is minimal. Nonetheless, the failure morphology between the two simulations is somewhat different, since it does not show facesheet disbonding in the former, while it does in the latter, Fig. 20. Overall, the core crushes in an identical manner, indicating that the bulk of the load and energy absorbed is attributable to the behavior of the core.

Two honeycomb crush load–displacement curves in the transverse directions, as well as the three shear curves were not measured experimentally, but borrowed from the literature [16] for a different core type and modified using supplier-provided data. The differences between the actual curves and these referenced ones are likely to be responsible for the observed differences in the load–displacement curve and energy absorption for the global assembly model.

Element size for the sub-component model is five times that of the element models. This difference in mesh size is a necessity associated with limitations on computational power available, and the need to maintain identical element sizes for the tie-break contact definition. While the 0.1 in. × 0.1 in. (2.5 mm × 2.5 mm) size element is very well suited for the MAT 54 model of the facesheets, which is highly mesh-sensitive, it is not possible to use such a fine mesh for the solid core, which is relatively mesh-insensitive. Keeping the same mesh density for the large assembly model yields an enormous number of elements, while using such a coarse mesh for the element-level simulations makes them highly inaccurate. A compromise between accuracy and solution needs to be found, and the 0.5 in. × 0.5 in. (12.7 mm × 12.7 mm) size elements provides it.

The machine used to run these simulations is a desktop Dell Precision PWS 380 Dual Core Pentium D, with a 3.2 GHz CPU and 4 GB of RAM. Simulation time changes dramatically according to the condition being modeled. For the three-point bend flexure model, the simulation requires approximately 23 min, for the honeycomb crush approximately 59 min, for the single-lap shear approximately 16 s, and for the full-scale assembly level model 120 min. An attempt was made to use a multiprocessor cluster to run the same simulations. Although computing time was greatly reduced, the results obtained were significantly different, and even showed different physical responses. The issue associated with different results obtained by running the same input deck using different computational machines is known to the experienced community of analysts [3], and is associated with the way the calculations are performed in large parallel computing platforms. Therefore the authors opted to use a coarser mesh size for the full-scale assembly model, rather than revising all previous simulations.

Lastly, all experimental results performed to support the analysis are generated at quasi-static rates, 1.0 in./min (25.4 mm/min). Nonetheless, the simulations are performed at dynamic rates, 150 in./s (3.81 m/s), or 9000 times faster. To ensure consistency, at least among simulations and experiments, the simulations should be run at quasi-static rates. Although this is somewhat possible for the element-level simulations, at the cost of long simulation times, it becomes impossible for the sub-component level simulation, even

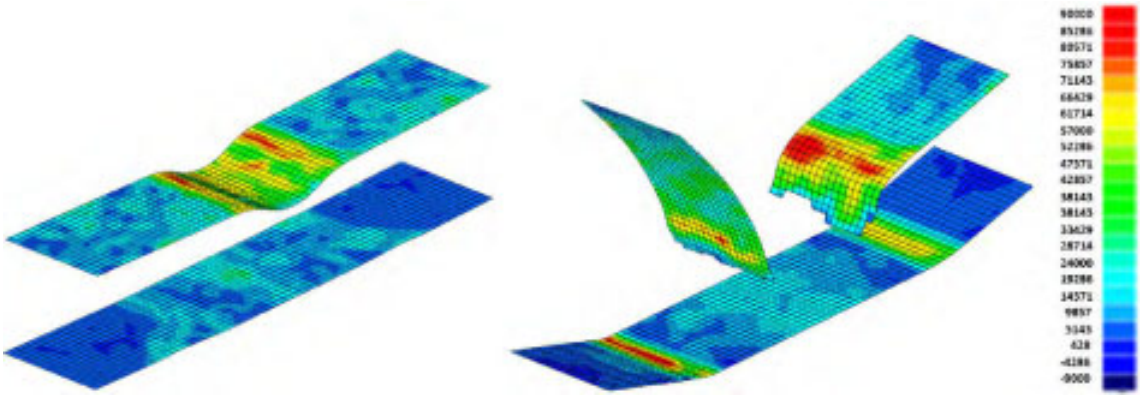

Fig. 19. Progression of facesheet damage and longitudinal stress contours during the last two time steps of Fig. 17; the core is removed for better visualization.

Fig. 20. Comparison between the morphologies of the simulation of the assembly at the end of the penetration test for the case with the measured adhesive strengths (left), the other with the reduced set of strengths (right).

utilizing a large cluster. Similar problems are being experienced by the participants in the CMH-17 round robin activity [3], where the simulations are dynamic, while all experimental results, both for material input property generation and for model validation, are obtained at quasi-static rates. Nonetheless, since final certification of the vehicle takes place at dynamic rates, identical to those of the simulations, it is instead recommended to keep all simulations in the dynamic regime, and change the rates at which the experiments are conducted. It is recommended to perform dynamic testing of the three-point bend flexure specimen, the honeycomb crush specimen, and the full-scale assembly penetration test. Although not trivial due to the large masses and relatively high velocities required, it is possible to perform these tests using a drop tower impact machine. However, generating high strain rate properties for the material models in not an easy task, as even performing a dynamic tension test is very difficult. Filtering of the results, as well as extrapolation of the true mechanical response for as simple a test as tension is challenging. In many cases great limitations exist on the size and shape of the specimen to be tested, such as in the Split Hopkinson Bar compressive test. For these reasons, the authors recommend, although aware of the implications, that quasi-static testing for this kind of problem only, may be sufficient to capture the relevant physical responses.

5. Conclusions

The building block approach can be used to simulate with success the problem of a deep sandwich panel being penetrated by a rigid pole. While several experiments are needed, at different levels of complexity, to generate material model input properties and to calibrate modeling parameters that cannot be measured by test, the approach enables the designer to develop accurate analytical models, thus reducing the number of tests required to be performed at the full-scale level. Commercial FE software LS-DYNA is used to successfully model all key aspects of the problem, including the composite facesheet flexural damage, honeycomb crushing, and adhesive disbonding. Analytical and experimental correlations of load–displacement curves, energy absorption, and global morphology of the failed specimen are very satisfactory. However, this kind of simulation has posed significant challenges for the analyst, who has been required to perform hundreds of runs to define, by trial-and-error, the optimal values for several modeling parameters. These calibration efforts need to be performed with systematic rigor and a constant effort to correlate them to physical quantities, in order to avoid losing all confidence in the predictive capabilities of the model. Predictive modeling increases safety, confidence in design, and is the foundation for the development of competitive technology and design.

Acknowledgments

The research was funded by Automobili Lamborghini S.p.A. The authors wish to thank Nicolo' Pasini, Casper Steenbergen, and Giulia Fabbri of Automobili Lamborghini for their contributions to the research. They would also like to thank Dr. Larry Ilcewicz, Allan Abramowitz and Curt Davies of the Federal Aviation Administration, as well as Al Miller, Patrick Stickler and Randy Coggeshall of The Boeing Co. for additional partial funding of this activity. Dr. Feraboli and Dr. Rassaian are the co-chairs of the CMH-17 (formerly MIL-HDBK-17) Crashworthiness Working Group. Many thanks to Karen Jackson of NASA Langley Research Center for spending many hours improving the paper before final publication.

References

[1] Feraboli P. Static strength determination of laminated composite materials within the current certification methodology for aircraft structures. J Aircraft, in press.
[2] MIL-HDBK-17. Building block approach for composite structures, vol. 3, Rev. F. West Conshohocken (PA): ASTM International; 2002 [chapter 4].
[3] Feraboli P, Rassaian M, Xiao X. Progress of the CMH-17 numerical round robin: year III. In: Proceedings of the 7th crashworthiness working group meeting, 54th CMH-17 coordination meeting. Salt Lake City (UT); March 2009.
[4] Deleo F, Wade B, Feraboli P, Rassaian M. Axial crushing of composite structures: experiment and simulation. In: AIAA 50th structures, dynamics and materials conference. CA: Palm Springs; May 2009 [Paper No. 2009-2532-233].
[5] Xiao X. Modeling energy absorption with a damage mechanics based composite material model. J Compos Mater 2009;43(5):427–44.
[6] Hallquist JO. LS-DYNA theoretical manual. Livermore (CA): LSTC; 2005.
[7] FMVSS Standard No. 214. Side impact protection, DoT/NHTSA 49 CFR. Par. 571.214, October 2004. p. 666–77 [chapter V].
[8] FMVSS Standard No. 214. Amending side impact dynamic test adding oblique pole test, US DoT/NHTSA Final Regulatory Impact Analysis; August 2007.
[9] ASTM D3039 standard test method for tensile properties of polymer matrix composite materials, vol. 15.03. West Conshohocken (PA): ASTM International; 2008.
[10] ASTM D6484 standard test method for open-hole compressive strength of polymer matrix composite laminates, vol. 15.03. West Conshohocken (PA): ASTM International; 2008.
[11] ASTM D5379 standard test method for shear properties of composite materials by the v-notched beam method, vol. 15.03. West Conshohocken (PA): ASTM International; 2008.
[12] ASTM D790 standard test methods for flexural properties of unreinforced and reinforced plastics and electrical insulating materials, vol. 08.01. West Conshohocken (PA): ASTM International; 2008.
[13] ASTM D7336 standard test method for static energy absorption properties of honeycomb sandwich core materials, vol. 15.03. West Conshohocken (PA): ASTM International; 2008.
[14] ASTM D1002 standard test method for apparent shear strength of single-lap-joint adhesively bonded metal specimens by tension loading, vol. 15.06. West Conshohocken (PA): ASTM International; 2008.
[15] Zhou Q, Mayer RR. Characterization of aluminum honeycomb material failure in large deformation compression, shear, and tearing. Trans ASME; 2002.
[16] Heimbs S, Middendorf P, Maier M. Honeycomb sandwich material modeling for dynamic simulations of aircraft interior components. In: Proceedings of the 9th international LS-DYNA users conference. Dearborn (MI); 2006.